Refereed Proceedings

The 13th International Conference on Fluidization - New Paradigm in Fluidization Engineering

Engineering Conferences International *Year* 2010

NUMERICAL STUDY OF BUBBLING FLUIDIZED BEDS: INFLUENCE OF IMMERSED TUBES, EXTRACTION METHODS AND AVERAGING PERIODS

Matthias Schreiber* Teklay Weldeabzgi Asegehegn† Hans Joachim Krautz‡

*Brandenburg University of Technology Cottbus, matthias.schreiber@tu-cottbus.de

†Brandenburg University of Technology Cottbus, Germany

‡Brandenburg University of Technology Cottbus, Germany

NUMERICAL STUDY OF BUBBLING FLUIDIZED BEDS: INFLUENCE OF IMMERSED TUBES, EXTRACTION METHODS AND AVERAGING PERIODS

Matthias Schreiber*, Teklay Weldeabzgi Asegehegn, Hans Joachim Krautz
Chair of Power Plant Technology, Brandenburg University of Technology Cottbus
Walther-Pauer-Strasse 5, 03046 Cottbus, Germany
* Tel.: +49 (0) 355 / 694006, Mail: matthias.schreiber@tu-cottbus.de

ABSTRACT

Numerical simulations using the Two Fluid Model were performed for 2D gas-solid fluidized beds with and without immersed horizontal tubes. The results were compared with experimental data available in the literature. Different techniques of extracting the time-averaged values of pressure drop and bed expansion and the influence of averaging time were investigated. Furthermore, the influence of tubes on the solids motion and distribution were studied.

INTRODUCTION

In industrial application bubbling fluidized beds containing immersed horizontal tubes play an important role, e.g. drying, combustion and FCC processes. The internal tubes have a significant influence on the bed properties and hence heat and mass transfer. Several researchers investigated the variation of fluidized bed hydrodynamics with internal tubes experimentally (1-4). Besides these experimental investigations CFD becomes more and more important in the field of fluidized bed research. Due to increasing computational capacities and powerful codes, numerical simulations allow to determine the complex phenomena in gas-solid flows. In general two main modeling approaches can be distinguished: the Discrete Particle Method (DPM) and the Two Fluid Model (TFM). The first one operates in the Euler-Lagrange framework and solves the equations of motion for each particle; for more details see e.g. Deen et al. (5). The second one treats the particles as a continuum (Euler-Euler approach) and needs additional empirical closures. DPM simulations are more accurate, but computationally more expensive and thus mainly applicable for lab-scale fluidized beds with a relatively small number of particles. TFM on the other hand is more suitable for engineering and industrial scales (van der Hoef et al. (6)). Previous studies showed that the TFM is able to predict the hydrodynamics of bubbling fluidized beds satisfactorily (7-9).
Bed expansion and pressure drop are important parameters in the design and scale up of fluidized beds. Though it is relatively easy to measure these properties using experiments, the way of extracting the time-averaged values from numerical simulations is not clear and usually not mentioned with the exception of Lindborg et al. (12). In addition a wide variation of averaging periods, e.g. ranging from 3 up to 18 seconds, were used for analyzing the time-averaged bed characteristics (7-11). These aspects could partially explain the still existing inconsistency between

experimental data and numerical results for fluidization problems. Therefore, in this paper the influence of extraction method and averaging time on the simulation results and the effect of different tube arrangements were investigated.

NUMERICAL MODELING

Governing Equations and Closures

For modeling the gas-solid flow the Euler-Euler Two-Fluid-Model was chosen due to the scale of the investigated systems and large number of particles. The commercial CFD-Code Fluent 6.3 (13) was used to solve the conservation equations of mass (a), gas (b) and solid (c) momentum and granular energy (d). By assuming only local generation and dissipation of granular energy, the so-called algebraic form (14) of the latter one was used in this work. For closing the set of governing equations, closure relations based on the Kinetic Theory of Granular Flow (KTGF) were applied (15). Tables 1 and 2 respectively show the closure models, and the physical properties and simulation parameters used in this study.

$$\frac{\partial(\varepsilon_q \rho_q)}{\partial t} + \nabla \cdot (\varepsilon_q \rho_q \mathbf{u}_q) = 0 \qquad \text{(q=g for gas and q=s for solid)} \qquad \text{(a)}$$

$$\frac{\partial(\varepsilon_g \rho_g \mathbf{u}_g)}{\partial t} + \nabla \cdot (\varepsilon_g \rho_g \mathbf{u}_g \mathbf{u}_g) = \nabla \cdot (\boldsymbol{\tau}_g) - \varepsilon_g \nabla P - \beta(\mathbf{u}_g - \mathbf{u}_s) + \varepsilon_g \rho_g \mathbf{g} \qquad \text{(b)}$$

$$\frac{\partial(\varepsilon_s \rho_s \mathbf{u}_s)}{\partial t} + \nabla \cdot (\varepsilon_s \rho_s \mathbf{u}_s \mathbf{u}_s) = \nabla \cdot (\boldsymbol{\tau}_s) - \varepsilon_s \nabla P - \nabla P_s + \beta(\mathbf{u}_g - \mathbf{u}_s) + \varepsilon_s \rho_s \mathbf{g} \qquad \text{(c)}$$

$$\frac{3}{2}\left(\frac{\partial(\varepsilon_s \rho_s \Theta)}{\partial t} + \nabla \cdot (\varepsilon_s \rho_s \mathbf{u}_s \Theta)\right) = (-P_s \mathbf{I} + \boldsymbol{\tau}_s) : \nabla \mathbf{u}_s - \nabla \cdot \mathbf{q} - \gamma - J \qquad \text{(d)}$$

Table 1: Closure models

Parameter	Model (Fluent)	Ref.
Solid viscosity	Syamlal-O'Brien	(14)
Solid bulk viscosity	Lun et al.	(16)
Frictional viscosity	Schaeffer	(17)
Frictional pressure	Johnson et al.	(18)
Solid pressure	Lun et al.	(16)
Radial distr. function	Lun et al.	(16)
Drag law	Gidaspow	(15)
	Syamlal	(14)

Table 2: Physical properties and simulation parameters

Parameter	Case A	Case B	Unit
Solid density	2500	2700	kg/m^3
Solid diameter	275	230	µm
Maximum solid packing limit	0.65	0.63	
Initial solid volume fraction	0.60	0.58	
Initial bed height	0.40	0.30	m
Superficial gas velocity	0.15-0.55	0.15-0.35	m/s
Gas density	1.23		kg/m^3
Gas viscosity	17.9		µPa·s
Angle of internal friction	28.5		°
Restitution coefficient	0.9		
Minimum friction solid volume fraction	0.5		

Geometry and Grid

In this paper two different bed geometries from literature were investigated. Figure 1 shows the setup of Taghipour et al. (7), who used a pseudo-2D bed with 1 m in height and 0.28 m width. Glass beads with an initial bed height of 0.4 m were used. For studying this case a uniform quadratic grid with a mesh size of 5 mm was generated. For the second case the no-tube, in-line and staggered arrangements from Hull et al. (4) were used. As an example the staggered one is

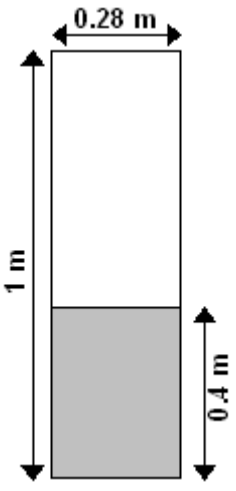

Fig. 1: Case A

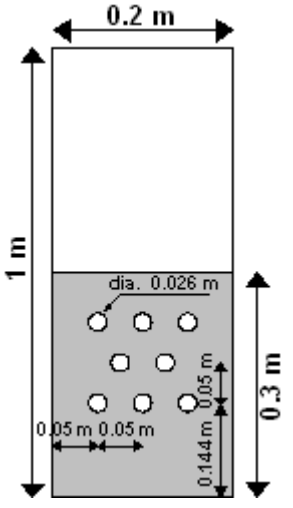

Fig. 2: Case B - staggered

drawn in figure 2. The grid of the no-tube case is also uniform quadratic with 5 mm size whereas the tubes cases were meshed with tri-elements starting from 5 mm near the tubes up to 8 mm in the freeboard region.

Boundary Conditions and Numerical Setup

For both geometries a pressure outlet boundary condition on top with a fully developed gas flow was assumed. At the walls and the surfaces of the tubes the no-slip conditions for the gas phase and partial slip conditions (18) with a specularity coefficient of 0.25 for the solid phase were applied. At the inlet a velocity inlet boundary condition with uniform velocity for the gas phase was used. Phase-Coupled SIMPLE was chosen for velocity-pressure coupling. The discretization was 1^{st} order implicit in time, 2^{nd} order upwind for momentum and QUICK for continuity. Time steps were 10^{-4} s giving good convergence with a residual criterion of 10^{-3}.

RESULTS AND DISCUSSION

Averaging Period

Due to the transient nature of bubbling fluidized beds bed properties are usually averaged over a certain period of time. To avoid the start-up effect and break the symmetric flow, the first few seconds have to be neglected. In this study the averaging time was started after 3 seconds of real flow time. For investigating the influence of averaging periods, plots of void fraction and vertical solid velocity (as the dominant component of solid motion) at different heights were compared using the geometry of case A. Figure 3 shows the different plots. The superficial velocity was 0.38 m/s, which is 6 times the minimum fluidization velocity (7).

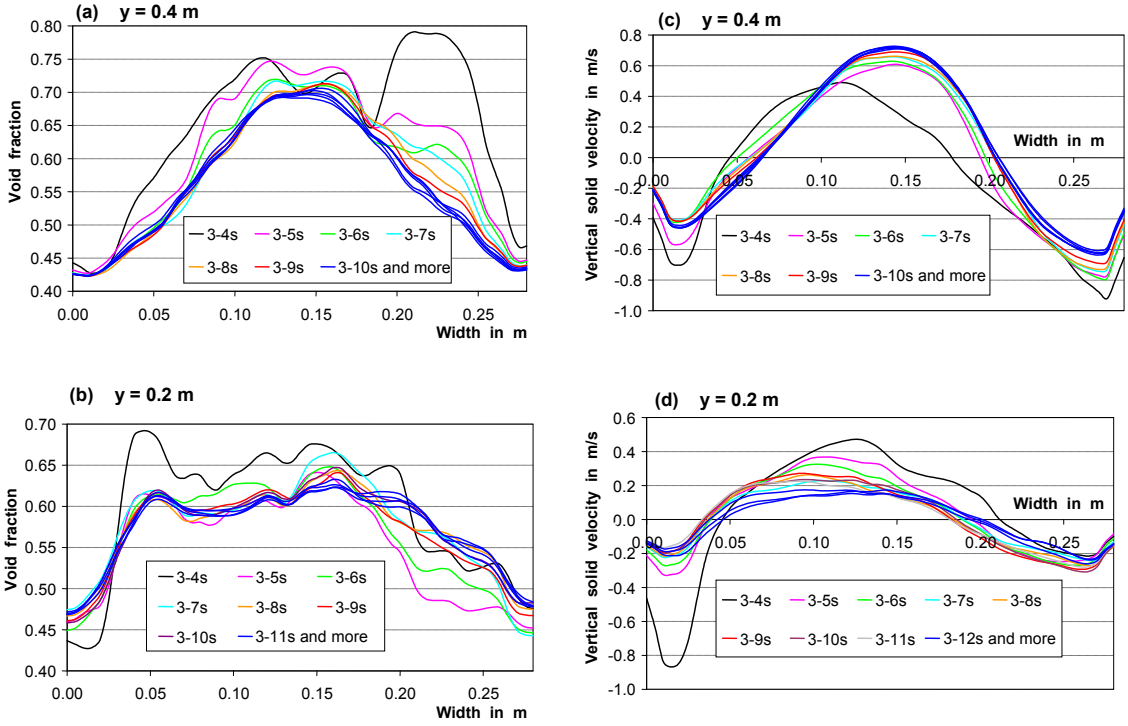

Fig. 3: Plots of time-averaged void fraction (a+b) and vertical solid velocity (c+d) at y=0.2 m and y=0.4 m

From the figures above it can be seen that the bed properties were very sensitive to the averaging period. Especially within the first few seconds the averaged values vary relatively strong. With increasing averaging time these fluctuations reduced and the mean value reached “steady state” values. In order to minimize the simulation effort it is important to find an optimum between accuracy and time consumption. For the presented case it was found that an averaging period of 8 seconds is satisfactory for analyzing the time-averaged bed properties. Increasing the averaging period further will lead to higher computational time with negligible improvement in accuracy of the numerical results. This behavior was seen for both investigated drag laws.

Extraction Methods

In order to investigate their influence, different methods of extracting pressure drop and expansion ratio from the simulations were studied and compared with experimental data given by Taghipour et al. (7). When the reference pressure in the freeboard region is set to zero, the static pressure of the gas-solid mixture at the bottom of the bed equals the pressure drop. After the conservation equations are completely solved and the resulting pressure field is averaged over time, the pressure drop can be easily extracted by area-averaging of the bottom line of cells (facet average). The second option is to use a linear extrapolation of the pressure versus bed height plot (linear regression). In figure 4 the pressure drops extracted with these two different methods are plotted against experimental data. Both give almost identical and constant values over the whole velocity range. This was seen for both drag laws and also fits to the general theory of fluidization. In general the differences between the extracted pressure drops were less than 2 % of the mean value. Though the pressure drop should remain constant above the minimum fluidization point, in the experimental data of Taghipour et al. (7) it continues to increase with superficial velocity. They didn’t explain the reason and it was the source of discrepancy with the simulation, figure 4.

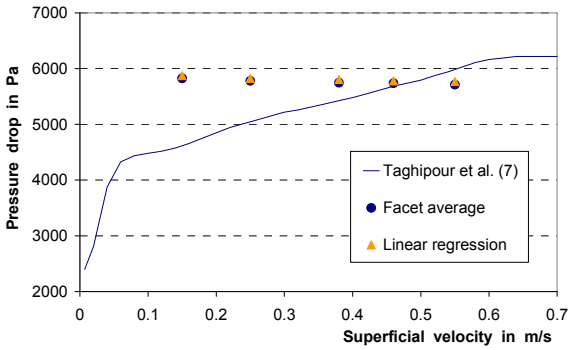

Fig. 4: Pressure drop versus superficial velocity

The extraction of the bed expansion ratio is more difficult than the pressure drop. It can be defined as the ratio of expanded bed height and static bed height. The difficulty here lies in the estimation of the expanded bed height during fluidization. One very often used method for experiments is shown in figure 5. Assuming a linear pressure drop with height, the intersection of this line with the abscissa gives the expanded bed height. Another possibility is to use the height at which the time-averaged

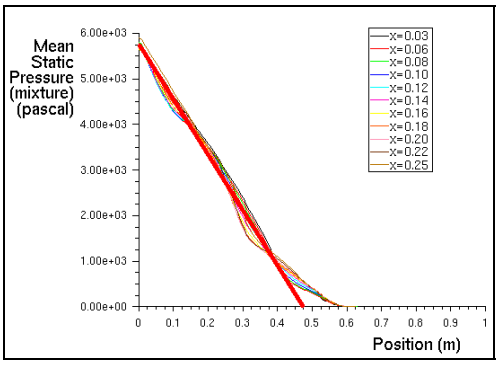

Fig. 5: Pressure versus bed height - linear regression

value of the bed pressure drop or the solid volume fraction drops below some certain limit. In this paper 0.1 % and 5 % of the maximum value of bed pressure drop and solid volume fraction were chosen. Figures 6 and 7 show these principles.

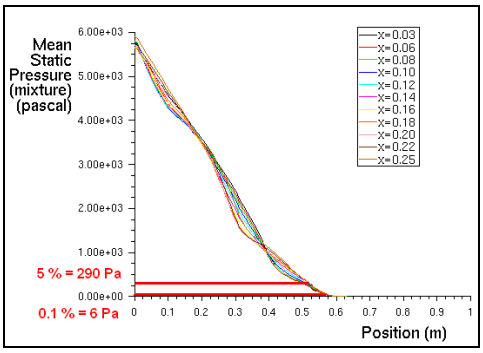

Fig. 6: Pressure versus bed height - pressure limit

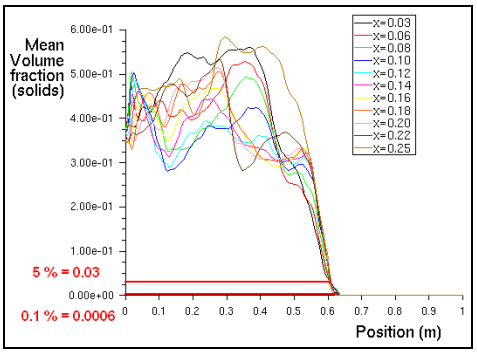

Fig. 7: Solid volume fraction versus bed height

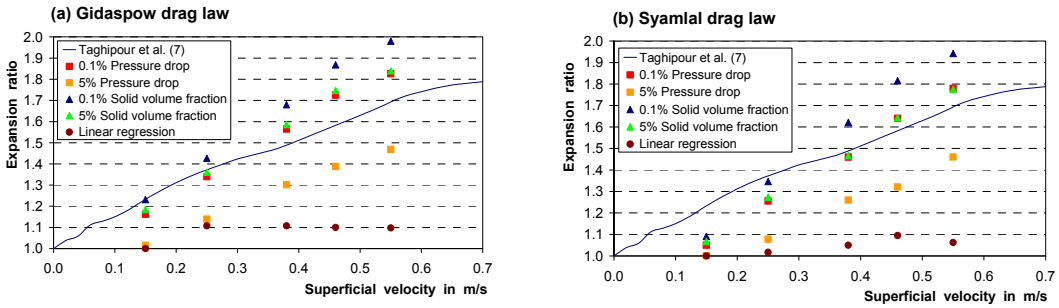

Fig. 8: Expansion ratio versus superficial velocity for Gidaspow (a) and Syamlal (b) drag law

Based on these definitions the results for the two drag models are summarized and compared in figure 8. The results showed that the extracted value of the expansion ratio was highly sensitive to the used method and deviations of more than 20 % may occur compared to the experimental data. For all methods the Syamlal drag model showed a slightly lower expansion than Gidaspow. This is consistent with findings of other researchers, e.g. Taghipour et al. (7). Over the whole velocity range both the 0.1 % pressure drop and 5 % solid volume fraction approach equally gave the results closest to experiment, but still with relatively large differences.

Tube Influence

For studying the influence of immersed horizontal tubes on the solid motion and distribution the arrangements of Hull et al. (4) were used. For all setups with and without tubes the simulations showed an average pressure drop of 4500 Pa with a deviation of less than 1.5 %. It was found that the chosen tube arrangements and drag laws had no major influence on the bed pressure drop. For the expansion ratio however, there were significant influences of the superficial velocities and drag laws. In table 3 the bed expansion ratios for the different cases are shown.

Table 3: Bed expansion ratio (H/H_{mf}) depending on tube arrangement and drag law

Superficial velocity	No tube		Staggered		In-line	
	Gidaspow	Syamlal	Gidaspow	Syamlal	Gidaspow	Syamlal
0.15 m/s	1.22	1.10	1.20	1.12	1.20	1.12
0.25 m/s	1.40	1.33	1.39	1.32	1.38	1.32
0.35 m/s	1.57	1.53	1.55	1.51	1.57	1.51

With increasing superficial velocity the bed expansion rises, which is well-known in fluidization theory. The Syamlal drag law showed a lower bed expansion than Gidaspow. Furthermore, the bed expansion was seen to be independent from the tube arrangement for the same superficial velocities and drag laws. From these results it can be concluded that the macroscopic bed properties pressure drop and expansion ratio are not influenced by the immersed tubes. The reason for this seems to be the small number of tubes, which was also reported by Olowson (2).

On the contrary, the influence of the tubes on the motion of solids was more significant. Figure 9 shows the time-averaged vertical solid velocity for the three tube arrangements right below the second row (y=0.18m), right above the second row (y=0.21m) and between the second and the third row (y=0.22m) for a superficial velocity of 0.25 m/s. For the no tube bed the vertical solid velocity increased with bed height, while this was not usually the case for the beds with internal tubes. For both tube arrangements the particles were observed to have higher vertical velocity between the tubes, where this was more pronounced for the in-line case. For the staggered arrangement relatively lower and uniform vertical velocities were observed. This is mainly due to the restriction of flow as the particles move upwards. For the in-line on the other hand they can move between the columns throughout the tube bank region without restriction which would give a higher vertical velocity.

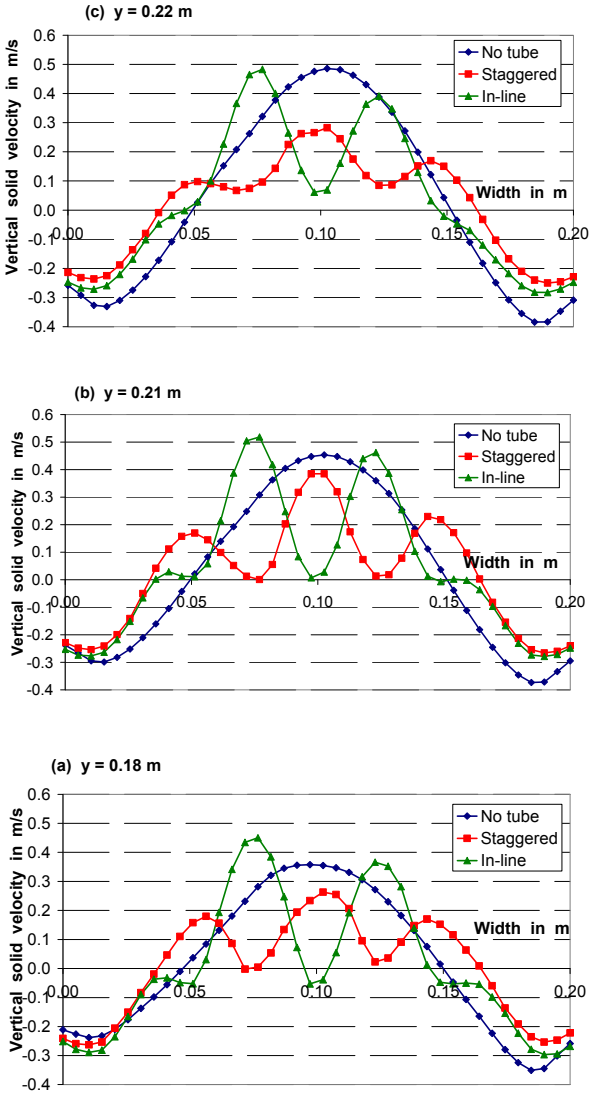

Fig. 9: Average vertical solid velocity versus width at y=0.18 m (a), y=0.21 m (b) and y=0.22 m (c)

Additionally, the bed-averaged vertical solid velocity for the two drag models are shown in figure 10. In general, the vertical solid velocity increases with the presence of tubes. While in the staggered case the velocity distribution is relatively uniform in the center and comparable with the no

tube one, the in-line case shows two peaks, which indicate channel-like flow in-between the tube columns. Regarding the drag laws, Gidaspow predicted higher vertical solid velocities than Syamlal.

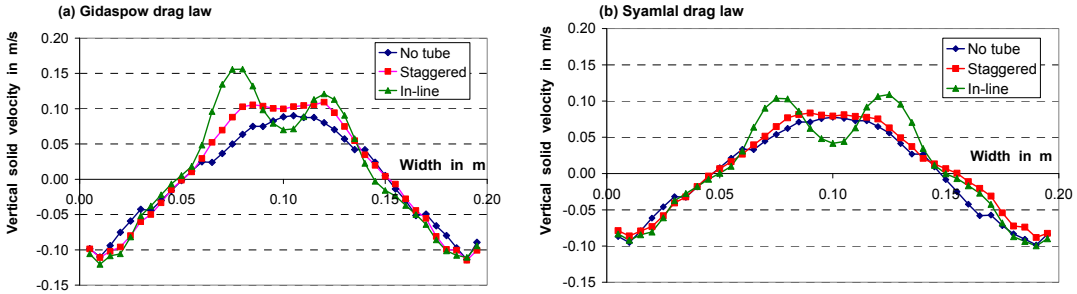

Fig. 10: Bed-averaged vertical solid velocity for Gidaspow (a) and Syamlal (b) drag law

In figure 11 the average solid volume fractions for all three arrangements are shown. The presence of tubes led to higher solid volume fractions near the walls and a more homogeneous distribution in the tube bank region. At the upper part of the tubes de-fluidized regions were observed, where the solids rested without moving. This can also be seen in figure 9b, where the solid velocities are zero at the position of the tubes. Moreover, the lower parts of the tubes were covered with gas pockets, which were seen as an additional source for bubble formation. These effects reduced with increasing superficial velocity.

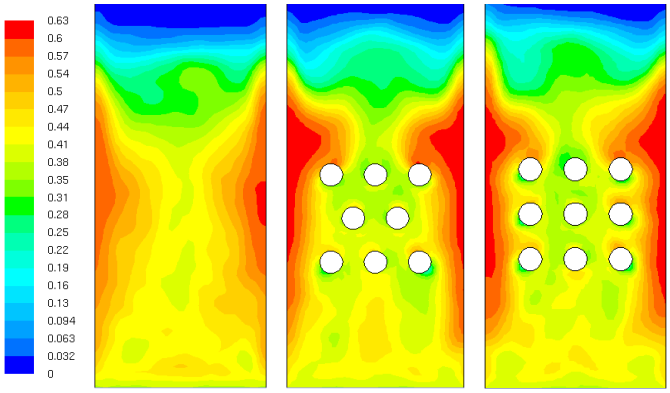

Fig. 11: Average solid volume fraction for no tube, staggered and in-line arrangement

CONCLUSION

Numerical simulations using the Euler-Euler Two Fluid Model (TFM) were performed for two dimensional gas-solid fluidized beds with and without immersed horizontal tubes. Different techniques of extracting the time-averaged values of pressure drop and bed expansion, and the influence of averaging time were investigated. Furthermore, the influence of tubes and drag laws on solid motion and distribution was studied. For the studied cases, it was found that an averaging period of less than 5 seconds lead to inaccuracy of results with 8 seconds to be an optimum taking into account the computational effort and accuracy of the results. Regarding the extraction methods pressure drops were less dependent while bed expansion showed greater variation with the way it was extracted. In this study better results were observed when the expanded bed height was defined at a height where the time average solid volume fraction drops below 5 % of the maximum or the pressure drop reached below 0.1 % of the overall pressure drop. Moreover the bed expansion was seen to vary with drag models. Investigations of the influence of tubes showed that immersed tubes significantly alter the solid motion and distribution, while they

slightly affect the pressure drop and bed expansion. In general the TFM in a promising tool for parametric investigations of fluidized beds. However, the way to extract bed properties could significantly influence the results which might lead to disagreements with experiments. Hence, an intensive study of the extraction methods is necessary to arrive at consistent and reliable methods. Moreover, further studies with more dense tube arrangements are required to clearly understand the influence of tubes on the fluidized bed hydrodynamics.

ACKNOWLEDGEMENT

The authors gratefully acknowledge the funding of this research project by the "Entrepreneurial Regions"-Initiative established by the German Federal Ministry of Education and Research and the International Graduate School supported by the Brandenburg University of Technology Cottbus and the Brandenburg Ministry of Higher Education, Research and Culture.

NOTATION

Symbols:

g	Gravitational acceleration, m/s^2
H	Bed height, m
I	Unit tensor
J	Fluctuating velocity-force correlation, $kg/(m^3s)$
P	Pressure, Pa
q	Granular energy diffusion, kg/s^3
t	Time, s
u	Velocity, m/s

Greek letters:

β	Interphase drag coefficient, $kg/(m^3s)$
γ	Dissipation of fluctuating energy, $kg/(m^3s)$
ε	Volume fraction
Θ	Granular temperature, m^2/s^2
ρ	Density, kg/m^3
τ	Shear stress tensor, N/m^2

Subscripts:

g	Gas phase
mf	Minimum fluidization
s	Solid phase

REFERENCES

1 Bouillard, J.X.; Lyczkowski, R.W.; Gidaspow, D.; 1989, AIChE Journal 35, p. 908-922
2 Olowson, P.A.; 1994, Chem. Eng. Sci. 49, p. 2437-2446
3 Olsson, S.E.; Wiman, J.; Almstedt, A.E.; 1995, Chem. Eng. Sci. 50, p. 581-592
4 Hull, A.S.; Chen, Z.; Fritz, J. W.; Agarwal, P. K.; 1999, Powder Technol. 103, p. 230-242
5 Deen, N.G.; van Sint Annaland, M.; van der Hoef, M.A.; Kuipers, J.A.M.; 2007, Chem. Eng. Sci. 62, p. 28-44
6 Van der Hoef, M.A.; van Sint Annaland, M.; Deen, N.G.; Kuipers, J.A.M.; 2008, Annu. Rev. Fluid Mech. 40, p. 47-70
7 Taghipour, F.; Ellis, N.; Wong, C.; 2005, Chem. Eng. Sci. 60, p. 6857-6867
8 Patil, D.J.; van Sint Annaland, M.; Kuipers, J.A.M.; 2005, Chem. Eng. Sci. 60, p. 73-84
9 Gustavsson, M.; Almstedt, A.E.; 2000, Chem. Eng. Sci. 55, p. 857-866
10 Rong, D.; Horio, M.; 2001, Int. J. Multiphase Flow 27, p. 89-105
11 Xie, N.; Battaglia, F.; Pannala, S.; 2008, Powder Technol. 182, p. 1-13
12 Lindborg, H.; Lysberg, M.; Jakobsen, H.A.; 2007, Chem. Eng. Sci. 62, p. 5854-5869
13 Fluent Inc.; 2006, FLUENT 6.3 User's Guide, 23.5 Eulerian Model Theory
14 Syamlal, M.; Rogers, W.; O'Brien; T. J.; 1993, MFIX Documentation Theory Guide, U.S. Dept. of Energy, DOE/METC-94/1004 (DE94000087)
15 Gidaspow, D.; 1994, Multiphase Flow and Fluidization: Continuum and Kinetic Theory Descriptions, Academic Press, Boston
16 Lun, C.K.K.; Savage, S.B.; Jeffrey, D.J.; Chepurniy, N.; 1984, J.Fluid Mech. 140, p. 223-256
17 Schaeffer, D.G.; 1987, J. Diff. Eq. 66, p. 19-50
18 Johnson, P.C.; Nott, P.; Jackson, R.; 1990, J.Fluid Mech. 210, p. 501-535